MM Science Journal | www.mmscience.eu
ISSN 1803-1269 (Print) | ISSN 1805-0476 (On-line)
Special Issue | TEAM 2024
Transdisciplinary and Emerging Approaches to Multidisciplinary Science
11.9.2024 – 13.9.2024, Ostrava, Czech Republic
DOI: 10.17973/MMSJ.2024_10_2024069

TEAM2024-00009

# ASSESSMENT OF GEOMETRIC DISTORTION OF CANTILEVERS PRINTED WITH DIFFERENT INTERNAL STRUCTURES AFTER DIFFERENT POST-PROCESSES

QUOC-PHU MA[1], MAREK SADILEK[1], PREETI GAUTAM[1*], MARTIN JANOSKO[1], JAKUB MESICEK[1]

[1]Department of Machining, Assembly and Engineering Metrology, Faculty of Mechanical Engineering, VSB-Technical University of Ostrava, 70833 Ostrava, Czech Republic

*Corresponding author; e-mail: preeti.gautam.st@vsb.cz

**Abstract**
This study assesses the geometric distortion of cantilevers fabricated from stainless steel 316L with varying internal structures using Selective Laser Melting (SLM) technology. The cantilevers were printed under identical conditions and subsequently post-processed with Wire Electrical Discharge Machining (WEDM) and heat treatment. The geometric deviations were evaluated using a micrometer and a Coordinate-Measuring Machine (CMM). This research underscores the importance of internal structure selection and post-processing in enhancing the geometric accuracy and mechanical stability of 3D-printed slender structures from stainless steel. By demonstrating that internal geometries can significantly influence the end product's structural performance, the findings provide valuable insights for the design and engineering of Additive Manufactured (AM) components, particularly in applications that involve bending.

**Keywords:**
Selective Laser Melting (SLM), Wire Electrical Discharge Machining (WEDM), heat treatment, 316L

## 1 INTRODUCTION

Additive manufacturing (AM) or 3D printing, has become a revolutionary force in contemporary manufacturing practices. This innovative method allows for the fabrication of intricate three-dimensional objects by depositing materials layer by layer, following precise digital instructions [Srivastava et al., 2023]. By enabling the production of complex geometries and minimizing material wastage, additive manufacturing is reshaping manufacturing processes across diverse sectors. The versatility of additive manufacturing extends beyond traditional subtractive methods, offering advantages in terms of cost-effectiveness and time efficiency. Through its capability to streamline prototyping processes and deliver customized designs, this technology presents opportunities for significant savings while enhancing the functionality of manufactured products [Mesicek et al., 2021]. The applications of AM methods are in aerospace (turbine blades, engine parts, and structural components), automotive (the fabrication of complex shapes, lightweight structures, and components), medical (producing patient-specific implants, prosthetics, and surgical instruments, architecture and construction, energy, defence and military industries [Mechali et al., 2024].

There are many types of AM technologies these include Material Jetting, Material Extrusion Binder Jetting, VAT Photopolymerization, Powder Bed Fusion including techniques like SLM, SLS, MJF, and EBM, Sheet Lamination, and DED [Dwivedi et al., 2023]. Among these methods, Selective Laser Melting stands out as one of the most prevalent processes, especially favored for fabricating high-performance components. Its widespread adoption is particularly notable in industries with stringent requirements, such as aerospace, automotive, and medical sectors [Sanchez et al., 2021].

Selective laser melting (SLM) is an AM technique that employs a high-powered laser to selectively dissolve and bond metallic powders layer by layer, resulting in the creation of a 3-dimensional object. Advantages of SLM processes, including the ability to produce components with highly intricate geometries that would be challenging or costly to create using traditional methods [Hajnys et al., 2020]. SLM presents a promising alternative to conventional production processes, offering several benefits such as streamlined production workflows, enhanced design flexibility, and reduced material wastage. The widespread adoption of SLM, particularly in industries like aerospace and automotive, is attributed to its ability to produce parts with more uniform microstructures and improved mechanical properties compared to conventionally manufactured components [Keaveney et al., 2020]. SLM-fabricated metal parts exhibit distinct characteristics, including residual porosity, surface roughness, anisotropic properties due to columnar grain structure, and significant tensile residual stresses near the surface layers [Huang et al., 2019]. These features, notably

the tensile residual stresses formed during the cooling phase of manufacturing, are considered pivotal factors contributing to distortion and potential delamination of the final products [Kaynak and Tascioglu, 2018].

Stainless steel 316L is widely utilized in SLM and is renowned for its outstanding corrosion resistance across various applications and environments. Numerous investigations have focused on the SLM method using SS316L due to its versatile applications [Mesicek et al., 2021, Gel'latko et al., 2022]. However, the mechanical properties of SS316L undergo significant changes under different SLM process conditions. Hence, it is imperative to study the mechanical characteristics of SLM-produced stainless steel 316L to ensure their safe usage and expand their application scope. Achieving precise geometric accuracy in AM components, particularly for delicate structures like cantilevers, presents a notable challenge due to distortions inherent in the printing process. These distortions, commonly observed in SLM, are exacerbated by thermal gradients and residual stresses stemming from the rapid heating and cooling cycles involved [Xie et al., 2022].

Extensive research has explored these factors, shedding light on the intricate mechanisms underlying geometric distortions in SLM-produced parts. Wang et al. [Wang et al., 2020], In additive manufacturing, distortion and residual stresses are significant challenges that adversely affect the dimensional accuracy and performance of the fabricated parts. Distortion refers to the deviation of the produced component from its intended shape or dimensions. Hemnath et al. [Anandan Kumar and Kumaraguru, 2019] Distortion can occur during the additive manufacturing process itself or when the fabricated part is detached from the substrate. Bartlett et al. [Bartlett and Li, 2019] The history of thermal cycling, numerous processing parameters, and intricate structures result in complex variations in distortion and residual stress. Several review articles have addressed the issue of residual stress in additive manufacturing. Jiang et al. [Jiang et al., 2020] post-processing methods like heat treatment and mechanical treatment are used to decrease distortion and residual stress in AM parts. Heat treatment, especially before support removal is effective but may cause unwanted grain growth and affect mechanical properties. Trevisan et al. [Trevisan et al., 2017], conducted a comprehensive examination of the primary process parameters and variables in Selective Laser Melting (SLM), concentrating on aluminum alloy and incorporating fundamental post-heat treatment. Additionally, the study underscores the importance of investigating novel heat treatment approaches for this SLM alloy. The internal configuration of a component significantly impacts its mechanical behavior and stability. Various lattice arrangements, such as gyroids, octet trusses, and honeycombs, have been studied for their potential to improve mechanical properties while minimizing weight [Borikar, Patil and Kolekar, 2023].

This study focuses on assessing the geometric distortion of cantilevers made from stainless steel 316L using SLM. By varying internal structures while maintaining consistent external dimensions and printing parameters, the research aims to explain the influence of internal geometry on overall geometric precision and mechanical stability. To enhance dimensional accuracy and mitigate residual stresses, post-processing methods like Wire Electrical Discharge Machining and heat treatment are applied. Existing literature underscores the intricate relationship between internal structure, post-processing techniques, and resultant geometric accuracy in SLM-fabricated parts. Although considerable advancement in understanding the mechanical and thermal dynamics of SLM, there remains a need for further investigation to optimize internal geometries and post-processing strategies. This research aims to add to this body of knowledge by investigate the geometric distortion such as beam thickness [mm], perpendicularity (PER) [mm], flatness (FLA) [mm], offset angle (ANG) [°] of stainless steel 316L cantilevers with diverse internal structures, providing fresh insights for the design and fabrication of precise AM components.

## 2 MATERIALS AND METHODS

### 2.1 Specimen design

The cantilever samples were chosen for the study whose geometry and dimensions can be found in **Figure 1**.

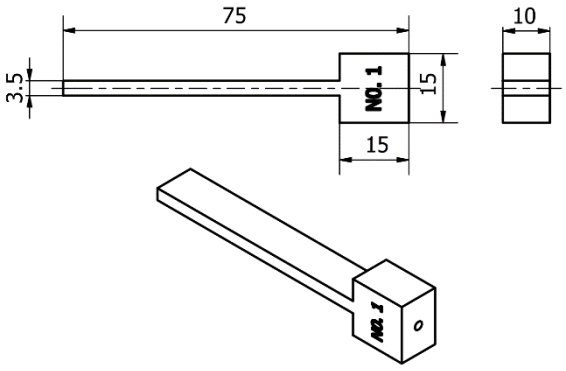


*Fig. 1: The cantilever design in mm.*

As can be observed in **Figure 1**, the cantilever has a slender beam section being the main subject of the study. There are four setups of internal structures, that is, 1) 100% infilled or full solid (100%); 2) 0% infill, or hollow with outer wall thickness of 0.5 mm (0%); 3) lattice type 1 (N.01) is type "Body diagonals with nodes rounded [MSG]" sizing of 2 mm; and 4) lattice type 2 (N.02) is type "diamond 30 percent relative density [MSG]" sizing of 2 mm. There are in total 12 samples for each setup, resulting in 48 samples in total. The lattice structures were designed using the Materialise Magics 22.0. software. The internal profiles of the cantilevers are illustrated in **Figure 2**.

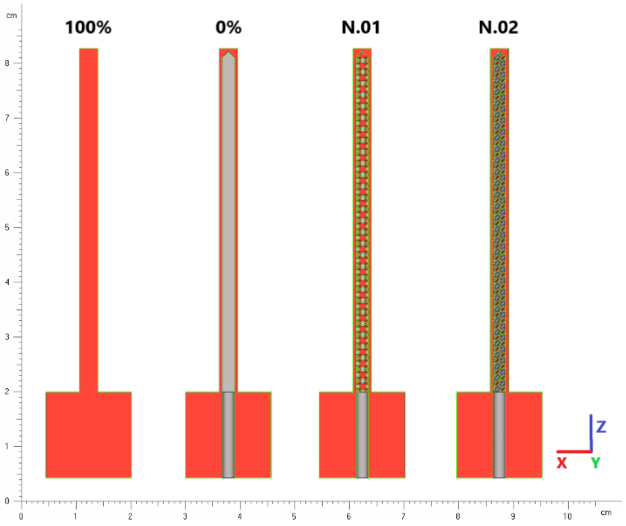


*Fig. 2: Different internal structures of the cantilevers.*

The samples were printed in vertical direction (Z direction) with an additional runway at the root of the slender beam

profile for samples with hollow profiles, so that the excess powder can be removed after printing.

### 2.2 Printing setup

The cantilevers were printed from stainless steel 316L using Renishaw - AM400 with a build space of 248 mm × 248 mm × 300 mm. The printing parameters are reported in **Table 1**. The parameters for printing and heat treatment were chosen carefully based on thorough pilot experiments. Initially, various parameters were tested to determine the most effective settings. After analysing the results of these preliminary trials, the parameters that yielded the best stability and performance were selected. This methodical approach ensured that the chosen parameters would optimize the printing and heat treatment processes, leading to higher quality and more reliable outcomes.

*Tab. 1: Printing parameters.*

| | |
|---|---|
| Laser power | 200 W |
| Scan speed | 650 mm/s |
| Layer thickness | 50 µm |
| Hatch spacing | 0.11 mm |
| Increment rotating angle | 67° |
| Preheat temperature | Ambient |

The printed cantilevers on the base plate are shown in **Figure 3**.

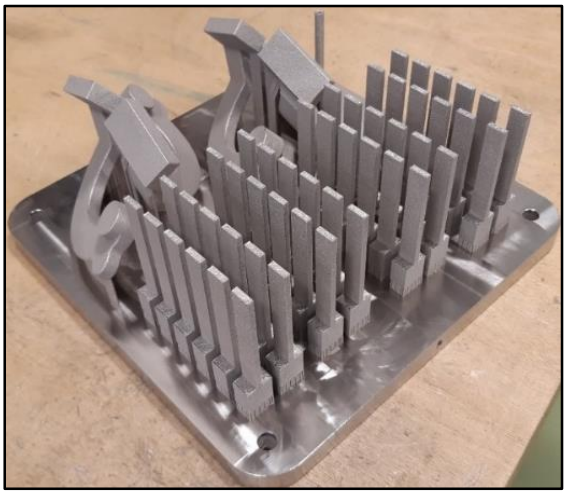

*Fig. 3: The distribution of the cantilevers on the base plate. The samples were printed in the front half and other samples on the other half to make use of the space.*

The samples were printed in the half front of the base plate together with other samples on the other half. It should be noted that the cantilevers were printed in the vertical direction to ensure the straightness of the slender beam profile. Supports were designed at the bottom of the cantilevers for better removal by saw.

### 2.3 Postprocess

The cantilevers were later subject to WEDM (machine CHMER G32F) and heat treatment of 550°C and 900°C (furnance LH120/12, Nabertherm GmbH) for an hour. The aim of WEDM cutting was to study the geometric change of the slender profile under additional material removal. On another hand, heat treatment has been proven to benefit the 3D printed metal parts by decreasing the residual stress [Mesicek et al., 2022]. Its impact on the geometric accuracy was as well investigated. In particular, samples after AM have 0.2 mm of the thickness cut from each side using WEDM. Samples after AM and heat treatment are cut with the thickness of 0.1 mm.

### 2.4 Measurement

For the evaluation of geometric accuracy, we investigated the beam thickness [mm], perpendicularity (PER) [mm], flatness (FLA) [mm], offset angle (ANG) [°]. The thickness measurements were conducted with micrometer while PER, FLA, and ANG were evaluated with Coordinate-Measuring Machine (CMM) (Wenzel LH65 CNC X3M Premium). The basis for measurements are illustrated in **Figure 4**.

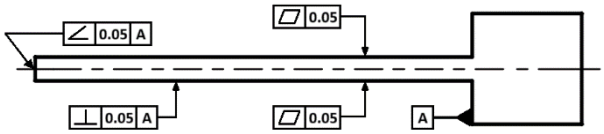


*Fig. 4: Basis for measurements.*

The offset angle is measured between the side of the beam section and base A. Each sample were measured three times and uncertainty level was calculated.

## 3 RESULTS AND DISCUSSION

The measurement results are listed in **Table 2** (thickness of the slender beam profile), **Table 3a** and **Table 3b** (PER, FLA, and ANG]. The thickness comparison among the samples is reported in **Figure 5**.

The thickness of AM samples in average is around 3.5 mm following the drawing in **Figure 1** with uncertainty level of approximately 0.25 mm. Regarding the samples which are subject to WEDM, their uncertainty level is slightly lower, approximately 0.23 mm. Their average thicknesses follow the aforementioned processes where AM/WEDM is around 3.1 mm (0.2 mm is removed from both sides), while AM/H550/WEDM and AM/H900/WEDM is around 3.3 (0.1 mm is removed from both sides).

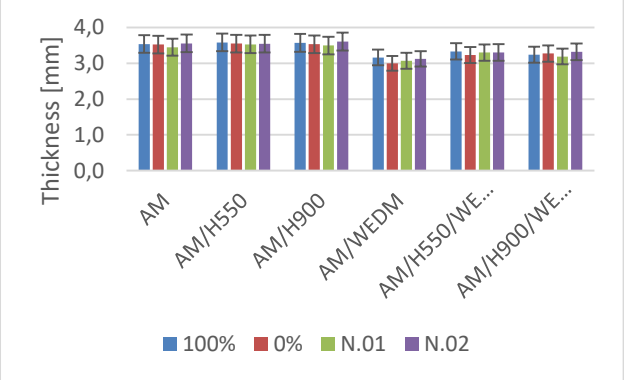


*Fig. 5: Thickness comparison.*

The deviation of the thickness can be up to ±0.1 mm as can be observed in **Figure 5** and data in **Table 2**. In addition, the results of PER, FLA, and ANG are respectively plotted in **Figure 6**, **Figure 7**, and **Figure 8**. It should be noted that, as opposed to **Table 3a** and **Table 3b**, the results are grouped according to PER, FLA, and ANG for better illustration and understanding the effect of the

postprocesses.

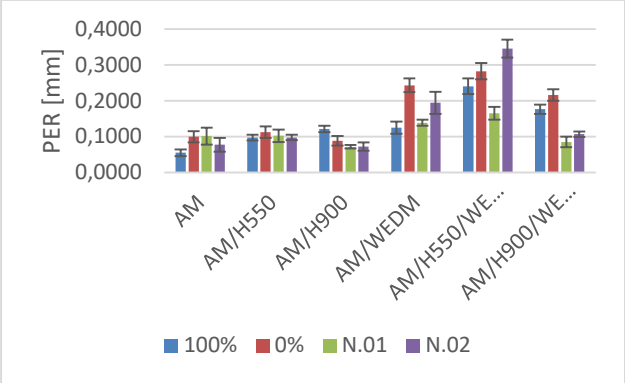


*Fig. 6: Perpendicularity comparison.*

As can be observed in **Figure 6**, the distortion in terms of perpendicularity is neglectable for samples that are at their as-built condition and after being heat-treated because of no geometric changes. For samples subjected to WEDM cutting, there is a noticeable higher PER measure. The difference can be explained by the alignment of the samples with respect to the wire during cutting. It is worth noting that the samples that are with 100% of infill and N.01 are in general with lower PER measure due to the fact that they are more stable given their structure.

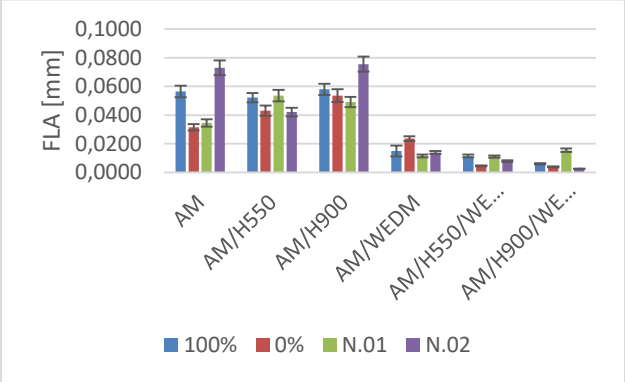


*Fig. 7: Flatness comparison.*

From **Figure 7**, we can see that samples AM and AM/H550 are in general with higher FLA which can be explained by the fact that the as-built surface is characterized with layers or so-called staircase effect. After WEDM cutting, it is undoubtedly that the surfaces have been flattened, resulting in significantly better FLA measurements. The heat treatment, indeed, do not offer any noticeable changes to FLA.

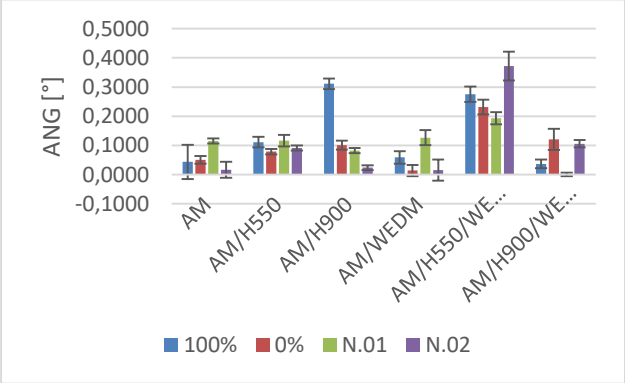


*Fig. 8: Offset angle comparison.*

In **Figure 8**, it stands out that there is a remarkable variation for offset angle ANG. This is because for measurements with such small angles, the associated uncertainty is relatively significant. An exception from the measurement is sample AM/H550/WEDM. This sample aligns with the PER results in **Figure 6** and FLA in **Figure 7**. It indicates that the two faces of the slender beam profile were well cut with WEDM, making FLA relatively low. However, its slender beam profile is tilted as well with respect to the base resulting in high PER and ANG measures. This can be considered an error with the post-process of four types of samples in the AM/H550/WEDM batch. The reason is applicable as well for significantly high ANG of sample 100% in AM/H900 batch.

## 4 CONCLUSIONS

This paper investigated the effect of heat treatment and WEDM as the two most common post-processing methods for SLM samples. The material under consideration is stainless steel 316L. Based on the obtained results, the following conclusions can be drawn:

- Heat treatment at 550°C and 900°C do not lead to noticeable geometric distortion of the samples. This indicates heat treatment can be employed for residual stress reduction without any concern about the geometric accuracy.
- WEDM introduces significant increase in the PER measure. The slender beam profile of the samples tilted more with respect to their bases.
- WEDM reduces significantly the layer effect on the printed samples. This is illustrated by the significantly lower FLA measure, which is a notable advantage of WEDM.
- Similar to PER control, ANG control with WEDM is not ideal because of the possible misalignment between the wire and samples. Therefore, for applications where angle accuracy is more important, post-processing with WEDM is not recommended. Instead, additional milling with CNC machine can be considered.
- There is no uniform and remarkable difference among the four types of internal structures for the slender beam profile in this study.

The results shed light on the effects of WEDM and heat treatment on the geometric accuracy of stainless steel 316L samples, which can help the designers to choose the appropriate postprocesses for their applications. For future works, the surface roughness of the samples as well as their strength under bending force can be considered.

## 5 ACKNOWLEDGMENTS

This study was conducted in association with the project Innovative and Additive Manufacturing Technology—New Technological Solutions for 3D Printing of Metals and Composite Materials (reg. no. CZ.02.1.01/0.0/0.0/17_049/0008407) financed by Structural Funds of the European Union. Article has been done in connection with project Students Grant Competition SP2024/087 „Specific Research of Sustainable Manufacturing Technologies“ financed by the Ministry of Education, Youth and Sports and Faculty of Mechanical Engineering VSB-TUO.

## 6 REFERENCES

[Anandan Kumar and Kumaraguru, 2019] Anandan Kumar, H. and Kumaraguru, S. (2019) ‘Distortion in metal additive manufactured parts’, 3D Printing and Additive Manufacturing Technologies, pp. 281–295.

[Bartlett and Li, 2019] Bartlett, J.L. and Li, X. (2019) 'An overview of residual stresses in metal powder bed fusion', Additive Manufacturing, 27, pp. 131–149.

[Borikar, Patil and Kolekar, 2023] Borikar, G.P., Patil, A.R. and Kolekar, S.B. (2023) 'Additively manufactured lattice structures and materials: present progress and future scope', International Journal of Precision Engineering and Manufacturing, 24(11), pp. 2133–2180.

[Dwivedi et al., 2023] Dwivedi, S. et al. (2023) 'A novel additive texturing of stainless steel 316L through binder jetting additive manufacturing', International Journal of Precision Engineering and Manufacturing-Green Technology, 10(6), pp. 1605–1613.

[Gel'atko et al., 2022] Geľatko, M. et al. (2022) 'Eddy current testing of artificial defects in 316l stainless steel samples made by Additive Manufacturing Technology', Materials, 15(19), p. 6783. doi:10.3390/ma15196783.

[Hajnys et al., 2020] Hajnys, J. et al. (2020) 'Influence of scanning strategy parameters on residual stress in the SLM process according to the bridge curvature method for AISI 316L stainless steel', Materials, 13(7), p. 1659.

[Huang et al., 2019] Huang, W. et al. (2019) 'Heat treatment of Inconel 718 produced by selective laser melting: Microstructure and mechanical properties', Materials Science and Engineering: A, 750, pp. 98–107.

[Jiang et al., 2020] Jiang, X. et al. (2020) 'Heat treatment effects on microstructure-residual stress for selective laser melting AlSi10Mg', Materials science and Technology, 36(2), pp. 168–180.

[Kaynak and Tascioglu, 2018] Kaynak, Y. and Tascioglu, E. (2018) 'Finish machining-induced surface roughness, microhardness and XRD analysis of selective laser melted Inconel 718 alloy', Procedia Cirp, 71, pp. 500–504.

[Keaveney et al., 2020] Keaveney, S. et al. (2020) 'Investigation of process by-products during the Selective Laser Melting of Ti6AL4V powder', Additive Manufacturing, 36, p. 101514.

[Mechali et al., 2024] Mechali, A. et al. (2024) 'ABRASIVE SURFACE TREATMENT OF ALSI10MG PARTS MADE BY L-PBF.', MM Science Journal [Preprint].

[Mesicek et al., 2021] Mesicek, J. et al. (2021) 'Abrasive surface finishing on SLM 316L parts fabricated with recycled powder', Applied Sciences, 11(6), p. 2869.

[Mesicek et al., 2022] Mesicek, J. et al. (2022) 'Effect of artificial aging on the strength, hardness, and residual stress of SLM AlSi10Mg parts prepared from the Recycled Powder', Materials Science and Engineering: A, 855, p. 143900. doi:10.1016/j.msea.2022.143900.

[Sanchez et al., 2021] Sanchez, S. et al. (2021) 'The creep behaviour of nickel alloy 718 manufactured by laser powder bed fusion', Materials & Design, 204, p. 109647.

[Srivastava et al., 2023] Srivastava, A.K. et al. (2023) 'Research Progress in metal additive manufacturing: Challenges and Opportunities', International Journal on Interactive Design and Manufacturing (IJIDeM), pp. 1–17.

[Trevisan et al., 2017] Trevisan, F. et al. (2017) 'On the selective laser melting (SLM) of the AlSi10Mg alloy: process, microstructure, and mechanical properties', Materials, 10(1), p. 76.

[Wang et al., 2020] Wang, K. et al. (2020) 'Study on defect-free debinding green body of ceramic formed by DLP technology', Ceramics International, 46(2), pp. 2438–2446.

[Xie et al., 2022] Xie, D. et al. (2022) 'A review on distortion and residual stress in additive manufacturing', Chinese Journal of Mechanical Engineering: Additive Manufacturing Frontiers, 1(3), p. 100039.

*Tab. 2: The measured thickness of the cantilever under different processes with different internal structure.*

| Process | 100% | 0% | N.01 | N.02 |
|---|---|---|---|---|
| AM | 3.5354 ± 0.2450 | 3.5204 ± 0.2440 | 3.4481 ± 0.2390 | 3.5538 ± 0.2462 |
| AM/H550 | 3.5813 ± 0.2488 | 3.5498 ± 0.2448 | 3.5265 ± 0.2462 | 3.5453 ± 0.2462 |
| AM/H900 | 3.2412 ± 0.2482 | 3.2714 ± 0.2448 | 3.1888 ± 0.2424 | 3.3196 ± 0.2498 |
| AM/WEDM | 3.1598 ± 0.2190 | 2.9972 ± 0.2076 | 3.0676 ± 0.2218 | 3.1238 ± 0.2164 |
| AM/H550/WEDM | 3.3319 ± 0.2308 | 3.2327 ± 0.2240 | 3.2990 ± 0.2286 | 3.3016 ± 0.2292 |
| AM/H900/WEDM | 3.5711 ± 0.2246 | 3.5309 ± 0.2266 | 3.4935 ± 0.2210 | 3.6011 ± 0.2300 |

*Tab. 3a: The evaluation of perpendicularity (PER), flatness (FLA), and angularity (ANG) with different internal structure.*

| | 100% | | | 0% | | |
|---|---|---|---|---|---|---|
| | PER [mm] | FLA [mm] | ANG [°] | PER [mm] | FLA [mm] | ANG [°] |
| AM | 0.0549 ± 0.0098 | 0.0564 ± 0.0040 | 0.0437 ± 0.0134 | 0.0996 ± 0.0156 | 0.0314 ± 0.0022 | 0.0507 ± 0.0588 |
| AM/H550 | 0.0973 ± 0.0084 | 0.0521 ± 0.0032 | 0.1112 ± 0.0096 | 0.1127 ± 0.0160 | 0.0431 ± 0.0036 | 0.0788 ± 0.0182 |
| AM/H900 | 0.1216 ± 0.0090 | 0.0579 ± 0.0040 | 0.3114 ± 0.0362 | 0.0884 ± 0.0132 | 0.0535 ± 0.0044 | 0.1012 ± 0.0148 |
| AM/WEDM | 0.1253 ± 0.0170 | 0.0148 ± 0.0038 | 0.0588 ± 0.0194 | 0.2433 ± 0.0192 | 0.0235 ± 0.0016 | 0.0141 ± 0.0218 |
| AM/H550/WEDM | 0.2406 ± 0.0218 | 0.0114 ± 0.0010 | 0.2758 ± 0.0250 | 0.2828 ± 0.0230 | 0.0045 ± 0.0004 | 0.2315 ± 0.0262 |

| | | | | | | |
|---|---|---|---|---|---|---|
| AM/H900/WEDM | 0.1765 ± 0.0132 | 0.0060 ± 0.0004 | 0.0364 ± 0.0152 | 0.2162 ± 0.0160 | 0.0038 ± 0.0004 | 0.1213 ± 0.0182 |

*Tab. 3b: The evaluation of perpendicularity (PER), flatness (FLA), and angularity (ANG) with different internal structure.*

| | N.01 | | | N.02 | | |
|---|---|---|---|---|---|---|
| | **PER [mm]** | **FLA [mm]** | **ANG [°]** | **PER [mm]** | **FLA [mm]** | **ANG [°]** |
| AM | 0.1014 ± 0.0238 | 0.0345 ± 0.0026 | 0.1154 ± 0.0090 | 0.0773 ± 0.0194 | 0.0730 ± 0.0052 | 0.0161 ± 0.0274 |
| AM/H550 | 0.1023 ± 0.0172 | 0.0535 ± 0.0040 | 0.1163 ± 0.0198 | 0.0977 ± 0.0078 | 0.0421 ± 0.0030 | 0.0913 ± 0.0090 |
| AM/H900 | 0.0716 ± 0.0050 | 0.0490 ± 0.0036 | 0.0826 ± 0.0060 | 0.0723 ± 0.0112 | 0.0755 ± 0.0052 | 0.0237 ± 0.0126 |
| AM/WEDM | 0.1389 ± 0.0890 | 0.0115 ± 0.0010 | 0.1267 ± 0.0255 | 0.1944 ± 0.0308 | 0.0138 ± 0.0010 | 0.0156 ± 0.0360 |
| AM/H550/WEDM | 0.1653 ± 0.0180 | 0.0110 ± 0.0008 | 0.1935 ± 0.0208 | 0.3462 ± 0.0250 | 0.0078 ± 0.0006 | 0.3721 ± 0.0494 |
| AM/H900/WEDM | 0.0851 ± 0.0148 | 0.0154 ± 0.0012 | 0.0004 ± 0.0090 | 0.1071 ± 0.0076 | 0.0025 ± 0.0001 | 0.1056 ± 0.0086 |